Regulation of Platelet Production: The Normal Response to Perturbation and Cyclical Platelet Disease

MOISÉS SANTILLÁN*†, JOSEPH M. MAHAFFY‡, JACQUES BÉLAIR*§
AND MICHAEL C. MACKEY‖¶

* Department of Physiology, Center for Nonlinear Dynamics in Physiology and Medicine, McGill University, Montreal, Quebec, Canada H3G 1Y6, † Esc. Sup. de Física y Matemáticas, Instituto Politécnico Nacional, 07738 México D.F., México, ‡ Department of Mathematical Sciences, San Diego State University, San Diego, CA 92182, U.S.A., §Département de Mathématiques et de Statistique and Centre de recherches mathématiques, Université de Montréal, Montréal, Québec, Canada H3C 3J7 and ‖ Departments of Physiology, Physics, and Mathematics, Centre for Nonlinear Dynamics in Physiology and Medicine, McGill University, 3655 Drummond Street, Room 1124, Montreal, Quebec, Canada H3G 1Y6

An age-structured model for the regulation of platelet production is developed, and compared with both normal and pathological platelet production. We consider the role of thrombopoietin (TPO) in this process, how TPO affects the transition between megakaryocytes of various ploidy classes, and their individual contributions to platelet production. After the estimation of the relevant parameters of the model from both *in vivo* and *in vitro* data, we use the model to numerically reproduce the normal human response to a bolus injection of TPO. We further show that our model reproduces the dynamic characteristics of autoimmune cyclical thrombobocytopenia if the rate of platelet destruction in the circulation is elevated to more than twice the normal value.

© 2000 Academic Press

1. Introduction

Periodic hematological diseases are unusual and fascinating since the numbers of one or more of the circulating blood cells spontaneously oscillate with periods on the order of days to months (Haurie *et al.*, 1998). They are classical examples of *dynamical diseases* (Glass & Mackey, 1988; Mackey & Glass, 1977). In some of these diseases, such as cyclical neutropenia (Haurie *et al.*, 1998, 1999a, b, 2000; Hearn *et al.*, 1998) and periodic chronic myelogenous leukemia (Fortin & Mackey, 1999), there is clear evidence for statistically significant cycling of all of the major blood cell groups with the same period in a given subject. It is generally thought that these disorders involve a destabilization at the hematopoietic stem cell (HSC) level leading to an oscillatory efflux of cells into all differentiation pathways (Mackey, 1978, 1979a, 1996). In other dynamic hematological diseases like periodic autoimmune hemolytic anemia (Bélair *et al.*, 1995; Kirk *et al.*, 1968; Mackey, 1979b; Mahaffy *et al.*, 1998; Orr *et al.*,

¶Author to whom correspondence should be addressed. E-mail: mackey@cnd.mcgill.ca

© 2000 Academic Press

1968) there is only an oscillation in one of the major blood cell types. Cyclical thrombocytopenia (CT) is a rare blood disease apparently falling into this second category.

Cyclic thrombocytopenia, in which platelet counts oscillate from normal to very low values, has been observed with periods between 20 and 40 days (Aranda & Dorantes, 1977; Balduini *et al.*, 1993; Bernard & Caen, 1962; Brey *et al.*, 1969; Caen *et al.*, 1964; Chintagumpala *et al.*, 1992; Cohen & Cooney, 1974; Dan *et al.*, 1991; Demmer, 1920; Engstrom *et al.*, 1966; Goldschmidt & Fono, 1972; Lewis, 1974; Skoog *et al.*, 1957; Tefferi *et al.*, 1989; Wasastjerna, 1967; Wilkinson & Firkin, 1966; Yanabu *et al.*, 1993) and reviewed by Cohen & Cooney (1974). Though it has been claimed that oscillations could be detected in the platelet counts of normal individuals with the same range of periods (Morley, 1969; von Schulthess & Gessner, 1986), this conclusion may not be statistically justified. The consensus seems to be that many cases of this disorder involve an auto-immune destruction of circulating platelets.

A few authors have formulated models for the regulation of thrombopoiesis (Eller *et al.*, 1987; Gray & Kirk, 1971; Györi & Eller, 1987; von Schulthess & Gessner, 1986; Wichmann *et al.*, 1979) assuming the existence of a negative feedback loop mediated by TPO. Bélair & Mackey (1987) specifically considered cyclical thrombocytopenia. They speculated that elevations in the random destruction rate of platelets could give rise to the characteristic patterns observed in cyclical thrombocytopenia. This paper considers this point in detail.

The outline of this paper is as follows. In Section 2, we give a brief summary of the normal physiology of platelet production and regulation, and an overview of the cyclical platelet pathologies. Section 3 develops an age-structured model consistent with the physiology of platelet production and the available data, and examines the steady-state relations that are important for the parameter estimation of Section 4. In Section 5, we numerically examine the behavior of the model with respect to recently published data on plasma TPO levels, and the response in normal individuals to TPO injection. Section 6 continues with an examination of autoimmune cyclical thrombocytopenia within the context of the model, and specifically as a response to elevated circulating platelet destruction rates. The paper concludes with a brief discussion in Section 7. Appendix A covers the numerical techniques that we used to investigate this age-structured model.

2. Normal and Pathological Platelet Production

2.1. PLATELET PRODUCTION AND CONTROL

Platelets mediate the body's clotting response to injury and day-to-day blood vessel repair, but the mechanism of platelet formation is complex and not fully understood. Platelets arise from large megakaryocytes found in the bone marrow, which are derived from hematopoietic stem cells. Mature megakaryocytes do not proliferate, but the megakaryocyte compartment is maintained by an approximately constant influx of progenitor cells (Branehog *et al.*, 1975). During the lifetime of the immediate precursor to the megakaryocyte, the megakaryoblast, mitosis ceases. With the cessation of mitosis, megakaryocytes begin to undergo nuclear endoreduplication—a process in which DNA replication occurs but the cytoplasm remains intact and the cell does not divide (Kuter *et al.*, 1997). The megakaryoblast nucleus grows and becomes lobulated. DNA replication usually occurs at least 3 times during the complete sequence of endoreduplication to yield a mature megakaryocyte of ploidy 16 (Kuter *et al.*, 1997) capable of platelet production (ploidy refers to the number of chromosomes per cell). Megakaryocyte ploidy, however, is variable and can be as high as 128 or 256 (Ellis *et al.*, 1995).

The immature megakaryocyte has a large nucleus that occupies most of the cell volume. As the ploidy increases, the cytoplasmic portion of the polyploid megakaryocyte expands. Parallel with this expansion comes the development of the smooth, internal demarcation membrane system that will eventually become the external membrane of each platelet. Once the demarcation membrane is in place, membrane-bound sections of cytoplasm are pinched off from the megakaryocyte to produce platelets (Beutler *et al.*, 1995). One mature megakaryocyte can give

rise to between 1000 and 5000 platelets (Beutler et al., 1995).

The primary cytokine responsible for platelet formation, thrombopoietin (TPO), was shown in 1994 to be the ligand for the c-Mpl receptor (Eaton & de Sauvage, 1997; Kaushansky, 1995; Papayannopoulou, 1996). Thrombopoietin stimulates hematopoietic stem cells to enter the cell cycle from their G_0 phase (Ritchie et al., 1996). TPO also stimulates proliferation and differentiation of megakaryocyte precursors (Tanimukai et al., 1997), decreases precursor apoptosis (Borge et al., 1996, 1997; Ratajczak et al., 1997; Ritchie et al., 1996, 1997; Zauli et al., 1997), promotes megakaryocyte maturation (Eaton & de Sauvage, 1997; Kaushansky et al., 1995), increases megakaryocyte ploidy (Kuter et al., 1997) and stimulates the release of platelets via the fragmentation of mature megakaryocytes (Kuter, 1996). The effects of TPO are synergistic with those of other cytokines (Zeigler et al., 1994). These effects of TPO qualitatively mimic the effects of erythropoietin and granulocyte colony stimulating factor in the erythroid and granulocytic lines, respectively. Whereas it was thought originally that the effects of thromobopoietin were limited to the cells of the megakaryocyte lineage, it is now known that in addition TPO plays a role in myelopoiesis and erythropoiesis and acts on both lineage committed cells and on the hematopoietic stem cells (Sitnicka et al., 1996; Solar et al., 1998; Yagi et al., 1999). TPO is thus both an early and a late acting factor in megakaryocyte differentiation (Kaushansky et al., 1995).

Human platelet levels normally remain relatively stable (Kuter et al., 1997), but platelet counts vary widely between species or between individuals within a species. The normal range for human platelet levels is $150–450 \times 10^9$ platelets l^{-1} blood with an average of 290×10^9 platelets l^{-1}. The body tightly regulates platelet mass and not platelet number, and TPO plays an important role in this regulatory process (Kuter, 1996).

2.2. CYCLICAL THROMBOCYTOPENIA

In cyclical thrombocytopenia, platelet counts oscillate from very low $(1 \times 10^9$ platelets l^{-1} blood) to normal $(150–450 \times 10^9 \, l^{-1})$ or above normal levels $(2000 \times 10^9 \, l^{-1})$. In addition, patients may exhibit a variety of clinical symptoms indicative of faulty coagulation. There are two proposed origins of cyclical thrombocytopenia. One is an auto-immune origin most prevalent in females. The other is of amegakaryocytic origin, more common in males.

Autoimmune cyclical thrombocytopenia is postulated to be an unusual form of idiopathic (immune) thrombocytopenic purpura (ITP) (Beutler et al., 1995). Autoimmune cyclical thrombocytopenia is characterized by a shortened platelet lifespan at the time of decreasing platelet counts (Beutler et al., 1995), consistent with an increase in platelet destruction, and normal to high levels of bone marrow megakaryocytes. In this type of cyclical thrombocytopenia the platelet oscillations are thought to be due to an elevated destruction rate of circulating platelets.

The second type of cyclical thrombocytopenia has a different etiology. In the amegakaryocytic variety platelet oscillations are thought to be due to a cyclical failure in platelet production (Bernard & Caen, 1962; Cohen & Cooney, 1974; Dan et al., 1991; Engstrom et al., 1966; Hoffman et al., 1989; Lewis, 1974). This variety is characterized by oscillations in bone marrow megakaryocytes preceding the platelet oscillations (Balduini et al., 1993; Bernard & Caen, 1962; Dan et al., 1991; Engstrom et al., 1966). Platelet lifespan is generally normal (Lewis, 1974) and antibodies against platelets are not detected (Hoffman et al., 1989). It is possible that the failure of platelet production could arise at the stem cell level since in at least one case (Kimura et al., 1996) there were parallel cycles of erythrocytes exactly out of phase with the megakaryocyte cycles. It is thought however, that in the majority of patients the cycling is at the megakaryocyte level (Dan et al., 1991; Hoffman et al., 1989).

Kimura et al. (1996) suggest that a cyclical fluctuation in the level of various cytokines is responsible for the oscillations in platelet counts. This group postulates that the fluctuation in cytokines leads to both cyclical platelet production and cyclical platelet destruction and thus both types of CT are involved simultaneously. It

is known that plasma concentrations of c-Mpl ligand are inversely proportional to circulating platelet numbers (Kuter & Rosenberg, 1995; Kuter, 1996) just as the circulating levels of granulocyte colony stimulating factor (G-CSF) are inversely proportional to circulating levels of granulocytes (Layton *et al.*, 1989). It has been suggested for both G-CSF (Layton *et al.*, 1989) and c-Mpl (Kuter, 1996) ligand that their levels are regulated by the mass of their primary cellular population targets (granulocytes and platelets, respectively).

Swinburne & Mackey (2000) examined patient data on 29 putative cyclical thrombocytopenia patients and three normal individuals, and were able to establish the existence of statistically significant cycling in 15 of the patients and all three of the normal individuals. They noted that those patients diagnosed as having autoimmune cyclical thrombocytopenia generally had shorter periods (range: 13–27 days) than those patients classified as amegakaryocytic (range: 27–65 days), and that the autoimmune patients generally showed platelet oscillations from normal to below normal, while the amegakaryocytic patients with the longer periods generally had oscillations from above normal to below normal. This observation, in conjunction with the results of this paper, lends support to the hypothesis that autoimmune and amegakaryocytic cyclical thrombocytopenia have a different dynamic origin.

3. Modeling Thrombopoiesis

The development of the mathematical model for thrombopoiesis follows our earlier age-structured mathematical models for erythropoiesis (Bélair *et al.*, 1995; Mahaffy *et al.*, 1998), bearing in mind that the primary difference between the processes of erythropoiesis and thrombopoiesis is in the development of the precursor cells. In erythropoiesis, the stem cells undergo rapid proliferation and differentiation until they reach the stage of reticulocytes, where the cells simply mature to become circulating erythrocytes. In thrombopoiesis, the stem cells proliferate, then become megakaryocytes that no longer proliferate, but undergo nuclear endoreduplication. As discussed in the previous section, these

megakaryocytes have different ploidy values at maturation and release differing quantities of platelets, which must be considered in the mathematical model.

Based on the relative frequencies of megakaryocytes in various ploidy classes (cf. Table 1), our age-structured model divides the megakaryocyte populations into three classes to simplify the calculations. Figure 1 provides an overview of the mathematical model. We begin our discussion of the model with the age-structured classes representing the megakaryocytes. Let $m_i(t, \mu)$, $i = 0, 1, 2$, represent the different ploidy classes of megakaryocytes with $i = 0$ corresponding to the ploidy values of 1, 2, and 4, $i = 1$ corresponding to the ploidy values of 8, 16 and 32, and $i = 2$ corresponding to the ploidy values of 64, 128, and 256. The time is t, and μ represents the age of the megakaryocyte. We assume that megakaryocytes age with unitary velocity so the boundary conditions at $\mu = 0$ for the three classes of megakaryocytes are

$$m_0(t, 0) = S_0(T), \qquad (1)$$

$$m_1(t, 0) = 0, \qquad (2)$$

$$m_2(t, 0) = 0, \qquad (3)$$

where all cells recruited from the stem cells enter the first ploidy class. Recruitment depends on the concentration of thrombopoietin, T, and is given by $S_0(T)$. The other ploidy classes can only receive new cells through nuclear endoreduplication from another ploidy class, which means that at $\mu = 0$ there are no new cells entering these compartments.

The partial differential equations describing the development of the megakaryocytes are given by

$$\frac{\partial m_0}{\partial t} + \frac{\partial m_0}{\partial \mu} = -k_0(T)m_0, \qquad (4)$$

$$\frac{\partial m_1}{\partial t} + \frac{\partial m_1}{\partial \mu} = k_0(T)m_0 - k_1(T)m_1, \qquad (5)$$

$$\frac{\partial m_2}{\partial t} + \frac{\partial m_2}{\partial \mu} = k_1(T)m_1, \qquad (6)$$
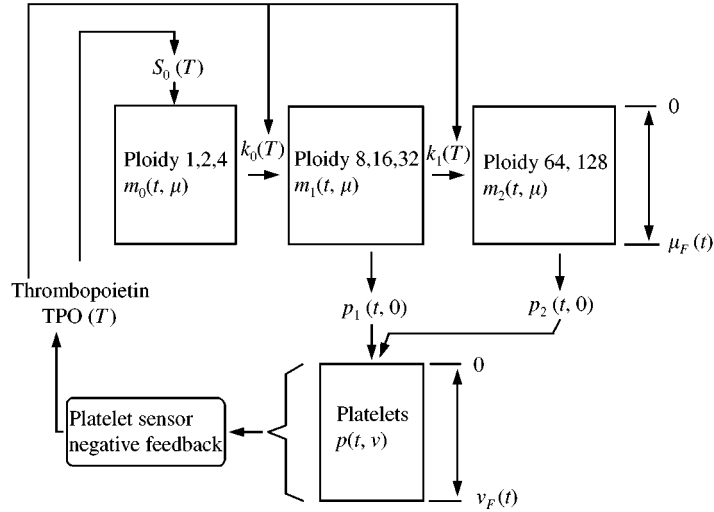
FIG. 1. A schematic of the age-structured model for thrombopoiesis.

where $k_i(T)$ is the transfer rate from ploidy class i to ploidy class $i + 1$. The domain for these partial differential equations is $t > 0$ and $0 < \mu < \mu_F$.

We assume that all megakaryocytes in ploidy classes larger than four mature to form platelets at age μ_F. Thus, the boundary conditions for the maturing megakaryocytes satisfy

$$W_1 m_1(t, \mu_F) = p_1(t, 0), \qquad (7)$$

$$W_2 m_2(t, \mu_F) = p_2(t, 0), \qquad (8)$$

where W_i is the average number of platelets produced by each megakaryocyte in the i-th class. Since the platelets are indistinguishable with respect to the megakaryocyte class from which they were derived, we simply examine the total age-structured platelet population. The new platelet production rate computed from eqns (7) and (8) satisfies

$$p(t, 0) = W_1 m_1(t, \mu_F) + W_2 m_2(t, \mu_F). \qquad (9)$$

Under the assumption that the platelet aging velocity is constant and unitary, the partial differential equation governing the age-structured platelet population is given by

$$\frac{\partial p}{\partial t} + \frac{\partial p}{\partial v} = -\gamma p, \qquad (10)$$

where γ is the random loss of platelets used in the normal repair of the tissues, especially the blood vessels. The domain for eqn (10) is $t > 0$ and $0 < v < v_F(t)$. The end point $v_F(t)$ of the domain is allowed to vary to account for changes in platelet lifespan. We use a constant flux boundary condition (similar to the one derived in Mahaffy et al. (1998)) given by

$$(1 - \dot{v}_F) p(t, v_F(t)) = Q, \qquad (11)$$

where Q is a fixed constant and equal to the total platelet mass removed at time t (cf. Mahaffy et al., 1998) for a careful derivation of eqn (11) and interpretation of Q).

There is a negative feedback mechanism for the control of platelets based on the total number (P) of circulating platelets. P is given by

$$P(t) = \int_0^{v_F(t)} p(t, v) \, dv.$$

This negative feedback control is mediated by the hormone thrombopoietin, T, whose concentration is assumed to satisfy the ordinary differential equation

$$\frac{dT}{dt} = f(P) - \kappa T. \qquad (12)$$

The function $f(P)$ represents the production of TPO, which is controlled by the total number of

platelets in the blood, and the last term $(-\kappa T)$ represents the random destruction of TPO. For computational purposes, we assume that $f(P)$ has the form

$$f(P) = \frac{a}{1 + KP^r}. \tag{13}$$

3.1. STEADY-STATE SOLUTION

This model is readily solved for the steady-state solutions. The stationary solutions (always denoted by a subscript $*$) for eqns (4)–(6) with the boundary conditions (1)–(3) are given in terms of the unknown functions $S_0(T)$, $k_0(T)$, $k_1(T)$ (which are not yet specified, but which will be determined in Section 4) by

$$m_{0*}(\mu) = S_0(T_*) e^{-k_0(T_*)\mu},$$

$$m_{1*}(\mu) = \frac{S_0(T_*)k_0(T_*)}{k_1(T_*) - k_0(T_*)} \left[e^{-k_0(T_*)\mu} - e^{-k_1(T_*)\mu} \right],$$

$$m_{2*}(\mu) = \frac{S_0(T_*)}{k_1(T_*) - k_0(T_*)}$$

$$\times \left[k_0(T_*) e^{-k_1(T_*)\mu} - k_1(T_*) e^{-k_0(T_*)\mu} \right.$$

$$\left. + k_1(T_*) - k_0(T_*) \right].$$

The total steady-state megakaryocyte count for each megakaryocyte class can be calculated from

$$M_i(T_*) = \int_0^{\mu_F} m_{i*}(\mu)\, d\mu, \quad i = 0, 1, 2.$$

After integration, we have the following:

$$M_0(T_*) = \frac{S_0(T_*)}{k_0(T_*)} \left[1 - e^{-k_0(T_*)\mu_F} \right], \tag{14}$$

$$M_1(T_*) = \frac{S_0(T_*)}{k_1(T_*)\left[k_1(T_*) - k_0(T_*)\right]}$$

$$\times \left[k_1(T_*) - k_0(T_*) + k_0(T_*) e^{-k_1(T_*)\mu_F} \right.$$

$$\left. - k_1(T_*) e^{-k_0(T_*)\mu_F} \right], \tag{15}$$

$$M_2(T_*) = \frac{S_0(T_*)}{k_0(T_*)\, k_1(T_*)\left[k_1(T_*) - k_0(T_*)\right]}$$

$$\times \left[k_1^2(T_*) e^{-k_0(T_*)\mu_F} - k_0^2(T_*) e^{-k_1(T_*)\mu_F} \right.$$

$$- k_0^2(T_*)k_1(T_*)\mu_F + k_0(T_*)k_1^2(T_*)\mu_F$$

$$\left. + k_0^2(T_*) - k_1^2(T_*) \right]. \tag{16}$$

Adding eqns (14)–(16), the total steady-state megakaryocyte population is

$$M(T_*) = \mu_F S_0(T_*).$$

The steady-state platelet population for the solutions of eqn (10) with boundary condition (9) yields

$$p_*(v) = p_*(0) e^{-\gamma v}, \tag{17}$$

where

$$p_*(0) = W_1 m_{1*}(\mu_F) + W_2 m_{2*}(\mu_F),$$

$$= \frac{S_0(T_*)\, W}{k_1(T_*) - k_0(T_*)}$$

$$\times \left[k_0(T_*)\, (e^{-k_0(T_*)\mu_F} - e^{-k_1(T_*)\mu_F}) \right.$$

$$+ \alpha(k_0(T_*) e^{-k_1(T_*)\mu_F} - k_1(T_*) e^{-k_0(T_*)\mu_F}$$

$$\left. + k_1(T_*) - k_0(T_*)) \right], \tag{18}$$

in which $W_1 = W$ and $W_2 = \alpha W$. Thus, α denotes the ratio of the number of platelets produced per megakaryocyte of class 2 to the number of platelets produced per megakaryocyte of class 1. The total platelet count in the steady state (P_*) is

$$P_* = \int_0^{v_{F*}} p_*(v)\, dv = \frac{1 - e^{-\gamma v_{F*}}}{\gamma}\, p_*(0). \tag{19}$$

Finally, in a steady state, eqn (12) gives

$$T_* = \frac{1}{\kappa} f(P_*) = \frac{1}{\kappa} \frac{a}{1 + KP_*^r}. \tag{20}$$

4. Parameter Estimation

The age-structured model for thrombopoiesis developed in Section 3 contains several unknown kinetic functions $[S_0(T), k_0(T), k_1(T)$ and $f(P)]$ and parameters $[\gamma, W_1, W_2, \mu_F,$ and $\kappa]$ that must be estimated. We also need equilibrium values of $T_*, P_*,$ and v_{F*} for normal subjects in order to numerically simulate the mathematical model and compare it with experimental and clinical data. In this section, we determine these functions and parameters from published experimental and clinical data.

4.1. TPO KINETICS

We begin with an analysis of the relationship between the circulating concentration of TPO, T, and the platelet count, P. Kuter (1996) reports experimental values of TPO concentration vs. platelet counts (both expressed relative to their normal steady-state levels) for sheep with different degrees of induced thrombocytopenia. Assuming that Kuter's experimental protocol established a quasi-steady state, and denoting the quasi-steady-state values of T and P by $\tilde{T}$ and $\tilde{P}$, respectively, then eqns (12) and (13) at the normalized steady-state values $\tilde{T}/T_*$ and $\tilde{P}/P_*$ gives a form appropriate for fitting the Kuter data:

$$\frac{\tilde{T}}{T_*} \simeq \frac{a}{\kappa T_*} \frac{1}{1 + (KP_*^r)\,(\tilde{P}/P_*)^r}. \quad (21)$$

A nonlinear least-squares fit of eqn (21) was performed, and Fig. 2 shows the experimental points and the best fit found by minimizing the error function with the routine `fmins` of `MatLab`. The values of the parameters a/κ, K, and r obtained from this procedure are

$$\frac{a}{\kappa} = 32.18\,T_*, \quad K = \frac{31.18}{P_*^r}, \quad \text{and} \quad r = 1.29,$$

which clearly depend on the equilibrium TPO (T_*) and platelet (P_*) values. As shown in Fig. 2, the interpolated function $f(P)$ gives a good fit to the TPO levels for platelet counts between zero and normal values.

Harker *et al.* (2000) measured the temporal evolution of the platelet count and the TPO concentration in human healthy volunteers
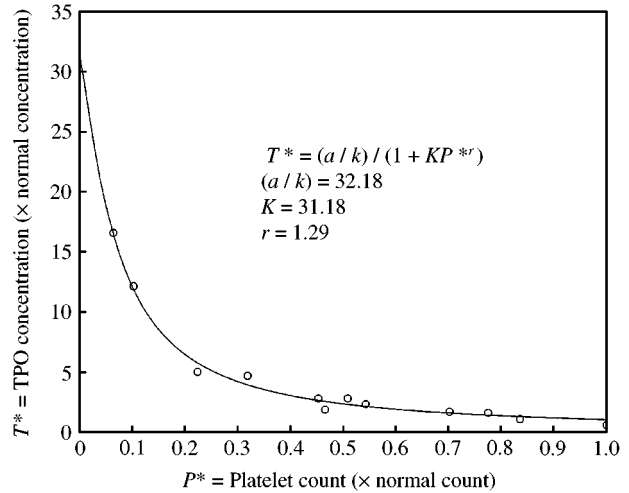

FIG. 2. Graph of TPO concentration as a function of platelet count showing the parameters that best fit the data of Kuter (1996).
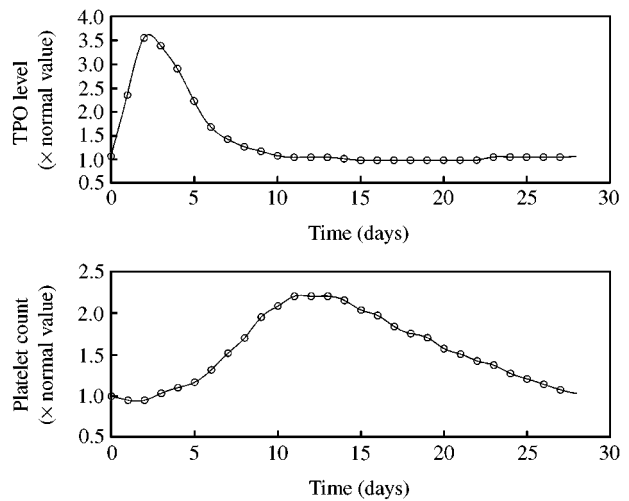

FIG. 3. Interpolated curves of the platelet count and TPO concentration experimental points, measured after a bolus administration of TPO in healthy human volunteers. From Harker *et al.* (2000).

receiving a bolus administration of TPO. The TPO concentration (T) and the platelet count (P) were interpolated at inter-medium times between the experimental points, using the `splines` algorithm of `MatLab`. The result of these interpolations is shown in Fig. 3.

The time derivative of T was calculated numerically using a forward Euler method. From these data and eqn (12) it is possible to estimate the TPO production rate function $[f(P)]$ for platelet counts larger than normal, given that,

according to Fig. 3, the effect of the TPO administration is to augment the platelet count above its normal value. We found by trial and error that a constant TPO production rate (independent of the platelet count) agrees with the Harker *et al.* data when the platelet level is greater than normal. In this case, eqn (12) can be replaced by

$$\frac{\mathrm{d}T}{\mathrm{d}t} = \kappa(T_* - T).$$

The left- and right-hand sides of this equation are calculated from the interpolation of T and its numerically calculated time derivative. They are plotted in Fig. 4, normalized by T_*. The value of κ was calculated to best fit both curves by minimizing the error function with the algorithm fmins of MatLab, using only times greater than five days after the administration of TPO to avoid pharmacokinetic effects. From this procedure, the TPO production function for platelet counts exceeding normal is given by

$$f(P_*) = \kappa T_*, \quad P_* < P,$$

allowing the estimation of the parameter κ to be

$$\kappa \simeq 0.54 \ \mathrm{day}^{-1}.$$

The parameter κ can also be estimated from other experiments. Vadan-Raj *et al.* (1997)
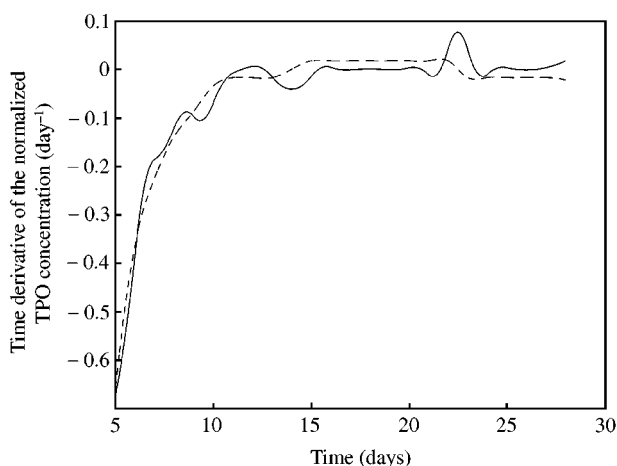

FIG. 4. Time derivative of the normalized TPO concentration, numerically calculated from the interpolated TPO concentration points (——), and calculated from the interpolated TPO concentration points as $\kappa(1 - T/T_*)$ (– – –). The value of $\kappa \simeq 0.54 \ \mathrm{day}^{-1}$ was calculated to provide the best fit to both curves. The original data are in Fig. 3.

measured serum thrombopoietin concentrations in humans after intravenous bolus administration of different TPO doses. They observe that plasma TPO concentration temporal decay is bi-exponential reflecting the presence of two time constants. The rapid early exponential can be attributed to the tissue absorption of TPO, and the second slower exponential is due to the active destruction of TPO. Only the second exponential is significant to our model. From these data, a TPO mean half-life between 20 and 25 hr is estimated. We took a half-life of 24 hr, from which the TPO destruction rate is $\kappa \simeq 0.69$ day^{-1}. This estimation of κ and the one from the data of Harker *et al.* (2000) are similar and we will use the first value since we are comparing our model behavior with other data from Harker *et al.* (2000).

Estimates for the equilibrium values T_* and P_* in normal subjects are available from a variety of sources. Kuter *et al.* (1997) report a TPO concentration of $0.022 \ \mathrm{U \ ml}^{-1}$ for the plasma of a thrombocytopenic sheep with a platelet count of 27% normal. From eqn (20) with the parameters estimated above, the TPO concentration in this case would be 4.75 times the normal value. Solving eqn (20) for the normal equilibrium TPO concentration gives

$$T_* = 0.005 \ \mathrm{U \ ml}^{-1}.$$

From Hoffbrand & Petit (1993, p. 300), the equilibrium value for the normal platelet levels in humans is

$$P_* = 2.5 \times 10^8 \ \mathrm{ml}^{-1}.$$

4.2. MEGAKARYOCYTE KINETICS

The parameter μ_F represents the maturation time for megakaryocytes. From the data of Camille & Marshall (1995), the megakaryocyte transit time in the bone marrow is 7 days, so

$$\mu_F = 7 \ \mathrm{days}.$$

Information on the functions $k_0(T)$ and $k_1(T)$ is obtained from experiments that determine distributions of ploidy classes as a function of TPO concentration. Equations (14)–(16) give the total megakaryocyte counts for our simplified

mathematical model, lumping together the ploidy classes into three compartments as depicted in Fig. 1. When normalized, the megakaryocyte counts in each class $M_i(T)$, $i = 0, 1, 2$, depend only on μ_F and the functions $k_0(T)$ and $k_1(T)$. We assumed that the $k_i(T)$ are functions of Michaelis–Menten type

$$k_i(T) = \frac{\alpha_i T}{1 + \beta_i T}, \quad i = 0, 1.$$

Broudy et al. (1995) have obtained in vitro experimental data on mouse megakaryocytes that provide distributions of ploidy classes as the concentration of TPO is varied. Their data were separated into the classes of our model, and a nonlinear least-squares fit to the data was performed, again by minimizing the error function with the routine fmins of MatLab. The resulting parameters are

$$\alpha_0 = 1.13 \times 10^{17} \, (\text{days} \times \text{U ml}^{-1})^{-1},$$

$$\beta_0 = 2.32 \times 10^{17} \, (\text{U ml}^{-1})^{-1},$$

$$\alpha_1 = 0.66 \, (\text{days} \times \text{U ml}^{-1})^{-1},$$

$$\beta_1 = 2.16 \, (\text{U ml}^{-1})^{-1}.$$

Note that the very large values of α_0 and β_0 imply $k_0(T)$ is effectively constant and gives $k_0(T) \simeq 0.485 \, \text{days}^{-1}$. Figure 5 shows the computed distributions for our model compared with the experimental results of Broudy et al. (1995).

The experiments reported by Broudy et al. (1995) were carried out in vitro. To test the feasibility of employing the estimations obtained from these data in our model, a comparison with other experiments carried out in vivo is useful. Harker et al. (2000) measured the relative frequencies of each megakaryocyte ploidy class in human bone marrow. Their results are presented in Table 1.

By lumping the ploidy classes as depicted in Fig. 1, it is possible to compare these experimental results with the megakaryocyte distributions calculated from the estimated functions $k_i(T)$, eqns (14)–(16), and the normal steady-state TPO concentration T_*. This comparison is shown in Fig. 6, and there is a qualitative agreement between the experimental megakaryocyte

distributions and those calculated from the model. Therefore, we conclude that, although calculated from in vitro experiments, the estimated functions $k_i(T)$ are reasonably accurate representations of the in vivo situation.

Pennington et al. (1979) measured nuclear and cell volumes in rat megakaryocytes of ploidy classes 8n, 16n, and 32n. The average nuclear and cell volumes were calculated for each cluster, and are given in Table 2.

The average cell volume and the average nuclear volume are linearly correlated. However, the average nuclear volumes roughly double between consecutive ploidy classes implying that the cell and cytoplasmic volumes must also double between consecutive ploidy classes. Platelets come from vesicles formed in the cell cytoplasm. It seems reasonable to assume that the number of platelets released per megakaryocyte is proportional to its cytoplasmic volume. From this and the above considerations, megakaryocytes of a given ploidy class should produce twice as many platelets as megakaryocytes of the preceding ploidy class. Therefore, the average number of platelets produced per megakaryocytes of our classes 1 and 2 can be calculated as

$$W_1 = \frac{N(p_8 + 2p_{16} + 4p_{32})}{(p_8 + p_{16} + p_{32})}$$

and

$$W_2 = \frac{N(8p_{64} + 16p_{128})}{(p_{64} + p_{128})},$$

respectively, where N is the average number of platelets produced per megakaryocyte of 8n ploidy class, and p_i ($i = 2, 4, 8, 16, 32, 128, 256$) is the relative frequency of each ploidy class under normal conditions (see Table 1). The parameter α, the ratio of the number of platelets produced per megakaryocytes of class 2 to the number of platelets reduced by megakaryocytes of class 1, is thus estimated as

$$\alpha = W_2/W_1 \simeq 4.2.$$

Assume that the megakaryocyte production function ($S_0(T)$) depends linearly on the TPO
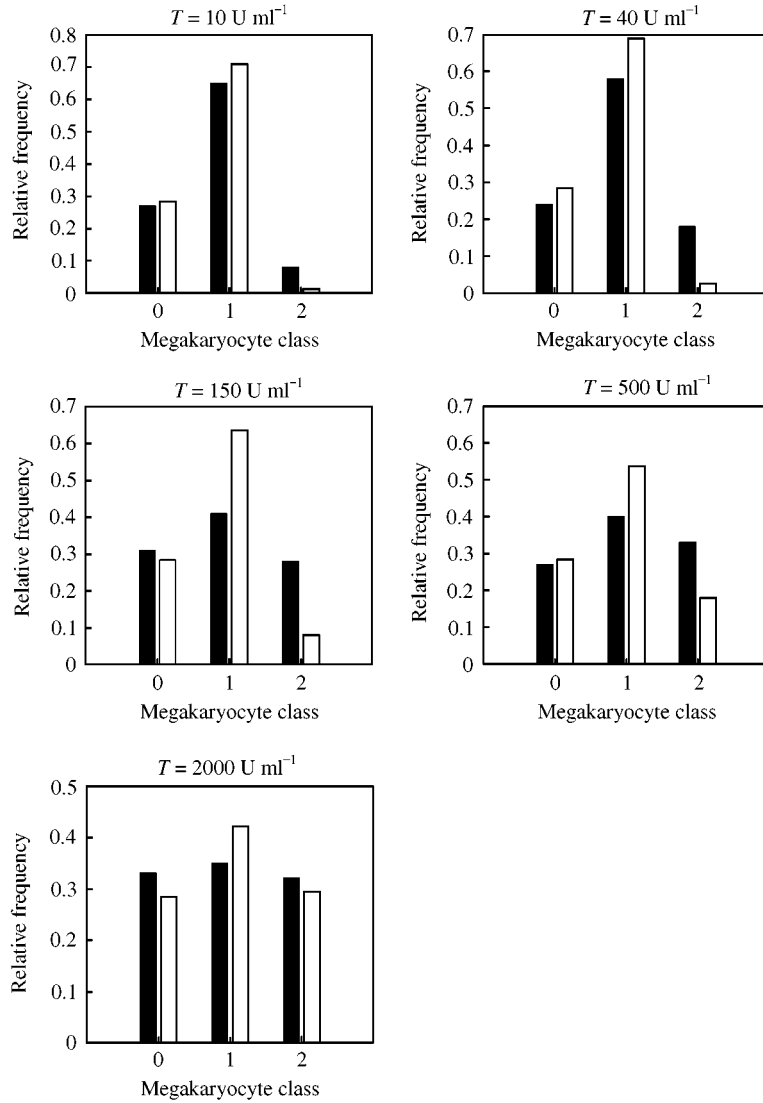
FIG. 5. The ploidy distribution of the model (□) and the experimental data (▮) of Broudy *et al.* (1995) for different concentrations of TPO.

TABLE 1

Relative frequencies of the different ploidy classes in human bone marrow megakaryocytes, taken from Harker et al. (2000)

Megakaryocyte ploidy class	Relative frequency
$2n$	0.06
$4n$	0.07
$8n$	0.19
$16n$	0.47
$32n$	0.2
$64n$	0.01
$128n$	0.0

concentration (T), i.e. $S_0(T) = S'_0 T$. Then from eqns (18) and (19)

$$\frac{\gamma}{1 - e^{-\gamma \nu_{F_*}}} = \frac{S'_0 T_* W}{k_1(T_*) - k_0(T_*)}$$

$$\times [k_0(T_*)(e^{-k_0(T_*)\mu_F} - e^{-k_1(T_*)\mu_F})$$

$$+ \alpha(k_0(T_*) e^{-k_1(T_*)\mu_F} - k_1(T_*) e^{-k_0(T_*)\mu_F}$$
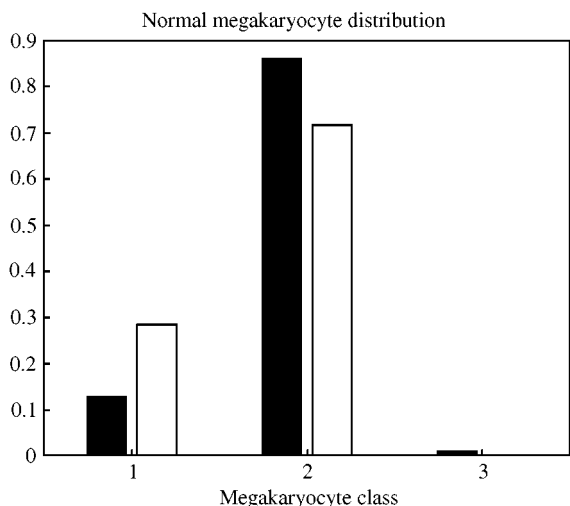
$$+ k_1(T_*) - k_0(T_*))].$$

FIG. 6. Comparison of experimental *in vivo* normal megakaryocyte distribution in humans (■, data from Harker *et al.* (2000)) and the megakaryocyte distribution calculated from the model with the normal TPO concentration (□).

TABLE 2

Average nuclear and cell volumes of megakaryocytes in the clusters identified by Pennington et al.
(1979)

Megakaryocyte ploidy class	Nuclear volume (fl)	Cell volume (fl)
$8n$	719.0	5568.18
$16n$	1573.03	10787.82
$32n$	2853.93	20927.29

From this, we can estimate the product $S_0'W$, since all other parameters are known (the parameter γ is estimated in the following subsection). After solving $S_0'W$ and performing the calculations we get

$$S_0'W \simeq 0.87 \ \text{day}^{-1} \times \frac{p_*}{T_*}$$

$$\simeq 9.35 \times 10^9 \, \text{day}^{-1} \times (\text{U ml}^{-1})^{-1} \times (\text{cells ml}^{-1}).$$

S_0' is the rate of production of new megakaryocytes per unit volume, per unit TPO concentration. Since megakaryocytes are not circulating cells, but reside in the bone marrow, the concentration of megakaryocytes is different from that of platelets. We therefore introduce a new volume unit V for the megakaryocyte

concentration by requiring that $S_0' = 1$ (cells V^{-1}) $\times (\text{U ml}^{-1})^{-1} \times \text{day}^{-1}$. With this,

$$W = 9.35 \times 10^9 \ \text{cells} \times \text{V} \times \text{ml}^{-1}.$$

Then we have

$$W_1 = W = 9.35 \times 10^9 \ \text{cells} \times \text{V} \times \text{ml}^{-1},$$

and

$$W_2 = \alpha W = 3.93 \times 10^{10} \ \text{cells} \times \text{V} \times \text{ml}^{-1}.$$

These values of W_1 and W_2 can be viewed as the average number of platelets produced per megakaryocyte of classes 1 and 2, respectively, times the factor that stands for the difference of concentration levels between the bone marrow and the blood stream.

4.3. PLATELET KINETICS

Circulating platelet kinetics are usually investigated using radioactive labeling. If it is assumed that only the circulating platelets are labeled, that they are in a steady state, and that there is no input of new labeled platelets, then our model predicts that the fraction of labeled platelets surviving in the blood at a time t after labeling is given by

$$\rho(t) = e^{-\gamma t} \frac{1}{1 - e^{-\gamma v_{F*}}} - \frac{e^{-\gamma v_{F*}}}{1 - e^{-\gamma v_{F*}}}. \quad (22)$$

Harker *et al.* (2000) measured the fraction of ^{111}In labeled platelets at different times after being administrated to human volunteers. We fitted the theoretical survival curve given by eqn (22) to these experimental points. For this, the error curve was again minimized using the algorithm fmins of MatLab. The experimental data and the best-fit curve are shown in Fig. 7, corresponding to the parameters v_{F*} and γ given by

$$v_{F*} \simeq 9.5 \ \text{days}$$

and

$$\gamma \simeq 0.15 \ \text{day}^{-1}.$$

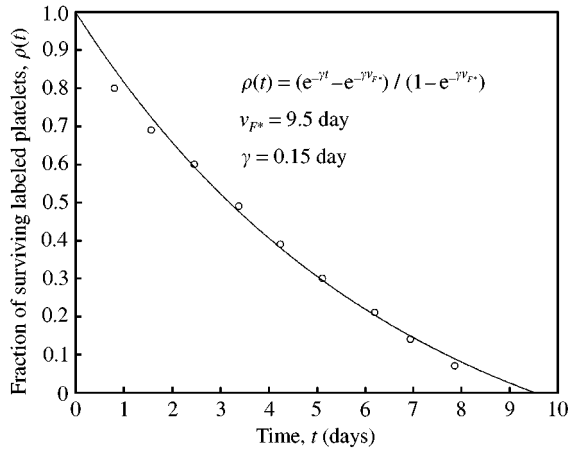The parameter Q can be calculated from eqn (11), which in the steady state implies that

FIG. 7. Fraction of surviving ^{111}In labeled platelets as a function of time. The experimental data from Harker *et al.* (2000) and the best-fitting curve predicted from the model are shown.

$Q = p_*(v_{F*})$, and from eqns (17) and (19):

$$Q = p_*(0)\,\mathrm{e}^{-\gamma v_{F*}} = \frac{\mathrm{e}^{-\gamma v_{F*}}}{1 - \mathrm{e}^{-\gamma v_{F*}}}\,\gamma P_*$$

$$= 0.0475 \ \text{day}^{-1}\, P_* \simeq 1.19 \times 10^7 \ \text{cells} \times \text{day}^{-1}.$$

5. Platelet Responses in Normal Humans

Harker *et al.* (2000) report experimental results concerning the dynamical effects of TPO stimulation on megakaryocytopoiesis, platelet production, and platelet viability in healthy humans. In those experiments, a single subcutaneous bolus injection of recombinant TPO ($3\,\mu\text{g}\,\text{kg}^{-1}$) was administered and the TPO concentration and the platelet count were measured daily for 28 days after the injection.

These experiments are simulated by solving the model system of equations as described in Appendix A and modifying the equation that determines the dynamics of the TPO concentration to

$$\frac{\mathrm{d}T}{\mathrm{d}t} = f(P) - \kappa T + I(t).$$

The function $I(t)$ accounts for the effects of the bolus injection on the concentration of TPO. We assume it has the form

$$I(t) = \begin{cases} A_I, & 0 \leqslant t \leqslant \varDelta_I, \\ 0 & \text{otherwise.} \end{cases}$$

This means that a constant amount of TPO, determined by A_I, is assumed to enter the blood stream during a time $\varDelta_I$ after the injection. Good agreement between the model and the experimental results is obtained with

$$A_I \simeq 1.9 \ \text{day}^{-1} \times T_*$$

and

$$\varDelta_I \simeq 3.2 \ \text{days}.$$

The values of all the other parameters are those estimated in Section 4. The initial conditions are those corresponding to the steady state.

The experimental results and the model simulations are shown in Fig. 8. The simulation reproduces the experimental results quite well. The parameter A_I determines the height of the peak in the TPO vs. time curve, while the parameter $\varDelta_I$ determines its position along the time axis. The shape of the peak and the decay rate after reaching its maximum, which are in good agreement with experiment, are properties determined by the model and the parameters. For the plot of the platelet count vs. time, the simulated response is completely determined by the modified model as described above. Although the model predicts platelet counts smaller than those measured between 5 and 10 days after the TPO injection,
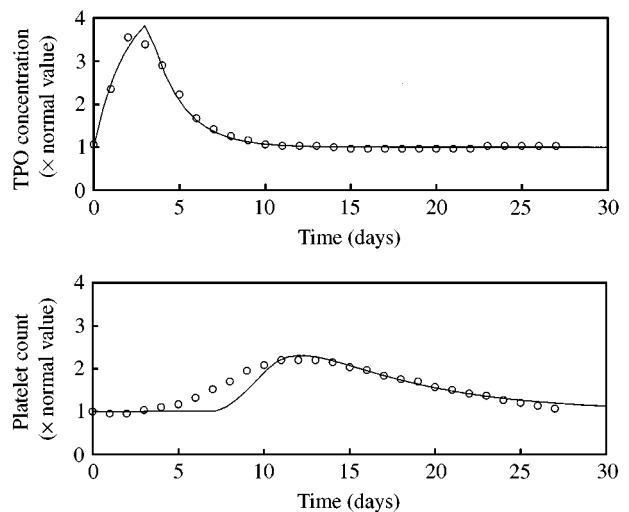

FIG. 8. Responses of the TPO concentration and the platelet count after a bolus intramuscular injection of TPO in healthy humans. Experimental results by Harker *et al.* (2000) (○), and the model simulation (——).

there is still good agreement between theory and experiment with respect to the amplitude of the response, the position of the maximum point, and the decay to the steady state.

6. Cyclical Thrombocytopenia

In Section 2.2, we discussed autoimmune and amegakaryocytic cyclical thrombocytopenia (Beutler *et al.*, 1995). Autoimmune cyclical thrombocytopenia is characterized by a shortened platelet lifespan at the time of decreasing platelet counts (Beutler *et al.*, 1995), consistent with an increase in platelet destruction, and normal to high levels of bone marrow megakaryocytes. In this type of cyclical thrombocytopenia the platelet oscillations are thought to be due to an elevated destruction rate of circulating platelets.

This can be simulated in the model by increasing the platelet destruction rate γ. We ran several numerical experiments with different values of γ, keeping all other parameters at the values estimated in Section 4. In all cases, the initial conditions were those of the normal steady state. The results show that for values of γ ranging from normal ($\gamma \simeq 0.15$ day^{-1}) up to $\gamma \simeq 0.34$ day^{-1}, the system reaches a stable steady state, characterized by a platelet count and platelet lifespan decreased from the corresponding normal values, while the TPO level and the total megakaryocyte count have values larger than normal. A typical example can be seen in Fig. 9, where the time evolution of the TPO level, the platelet count, the total megakaryocyte count and the platelet lifespan are shown for $\gamma \simeq 0.23$ day^{-1}.

For platelet death rates ranging from $\gamma \simeq 0.34$ to 1.65 day^{-1}, the steady-state number of platelets in the model is apparently unstable. The system displays sustained oscillations at the same frequency in all the variables, although their phase is different. The period of these oscillations decreases as γ increases, ranging from 22.3 days at $\gamma \simeq 0.34$ day^{-1} to 18.6 days at $\gamma \simeq 1.65$ day^{-1}. The amplitude of the oscillations in the platelet count is an increasing function of γ up to $\gamma \simeq 1.05$ day^{-1} and then decreases with further increase in γ. These maximum oscillations are
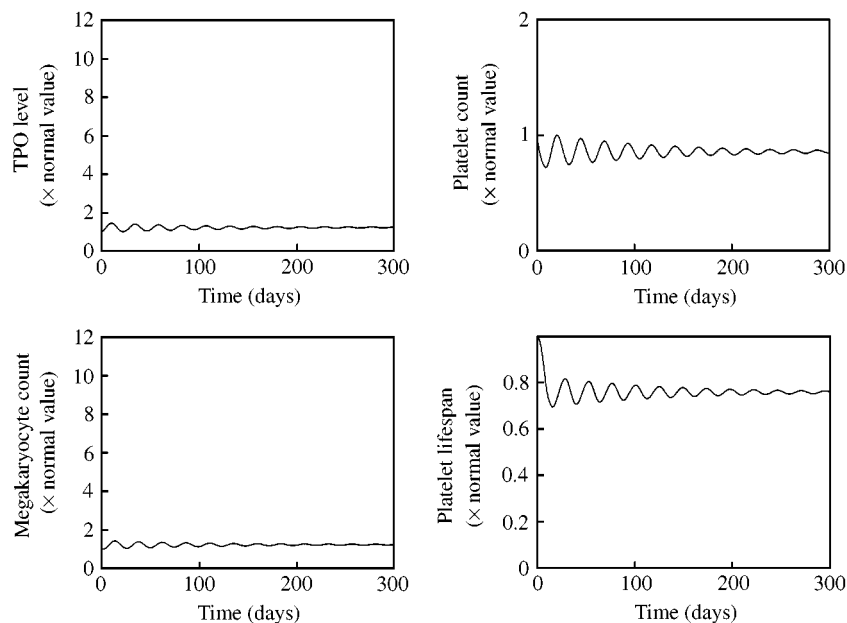

FIG. 9. Simulated time evolution of the TPO level, the platelet count, the megakaryocyte count, and the platelet lifespan in a "patient" with an increased platelet death rate (parameter γ). The model equations were numerically solved following the procedure described in Appendix A. The initial conditions were those of the normal steady state. All the parameters were set equal to their normal values, except for the platelet death rate which was set equal to 1.5 times the normal value ($\gamma \simeq 0.23$ day^{-1}). No transient was discarded. In this case the system evolves towards a stable steady state where the platelet count and the platelet lifespan are decreased below their normal values, while the megakaryocyte count and the TPO level are increased above their normal values.
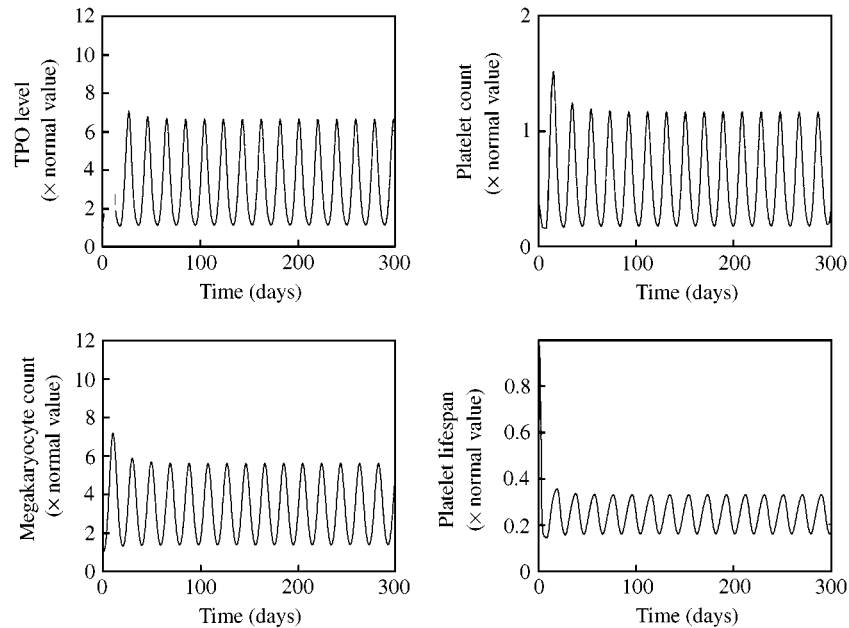
FIG. 10. Model response to an increased platelet death rate ($\gamma \simeq 1.05$ day^{-1}). All other conditions as in Fig. 9, except in this case, after a transient of about 100 days, the system reached a state with sustained oscillations in all the variables. The TPO level and the megakaryocyte count oscillate from about normal to higher levels, the platelet count oscillates from low to above normal values, and the platelet lifespan oscillates around a low value. The period of oscillation for all variables is about 19.4 days.

shown in Fig. 10. Note that the platelet count oscillates from a low of 0.415 up to 1.2 times the normal value. In this case, and in all others where sustained oscillations are seen numerically, the TPO level and the total megakaryocyte count oscillate from normal (or above normal) to higher values, while the platelet lifespan oscillates around a subnormal value.

For platelet death rates around $\gamma \simeq 1.5$ day^{-1}, the model displays behavior similar to that of autoimmune cyclical thrombocytopenia (Beutler *et al.*, 1995) as shown in Fig. 11. Thus, the TPO level and the total megakaryocyte count oscillate from slightly above normal to higher values, the platelet count oscillates from low (0.15 × normal) to normal values, the platelet lifespan oscillates around a decreased values (0.2 × normal), and the period of oscillation is around 18.8 days.

For values of γ larger than 1.65 day^{-1}, the system evolves again towards a stable steady state where both the platelet count and the platelet lifespan are significantly smaller than the corresponding normal values, while the TPO level and the megakaryocyte count values are increased above their normal values. An example of

this behavior is shown in Fig. 12 with $\gamma = 3.0$ day^{-1}.

This model for the regulation of platelet production is so complicated that we have as of yet been unable to complete a linear stability analysis. However, all of these numerical behaviors are identical with those observed in a qualitatively similar model for the control of red blood cell production (Mackey, 1979b). In that model there was a supercritical Hopf bifurcation induced by an increase in the death rate γ, followed by a reverse bifurcation that restabilized the steady state once γ became sufficiently large. Throughout this zone between these Hopf bifurcation points the period smoothly decreased as γ increased. This is precisely the behavior that we have seen in the present model.

7. Discussion

A mathematical model for the thrombopoiesis regulator system has been developed and investigated. The model assumes constant megakaryocyte and platelet aging velocities, considers only three lumped megakaryocyte classes, assumes
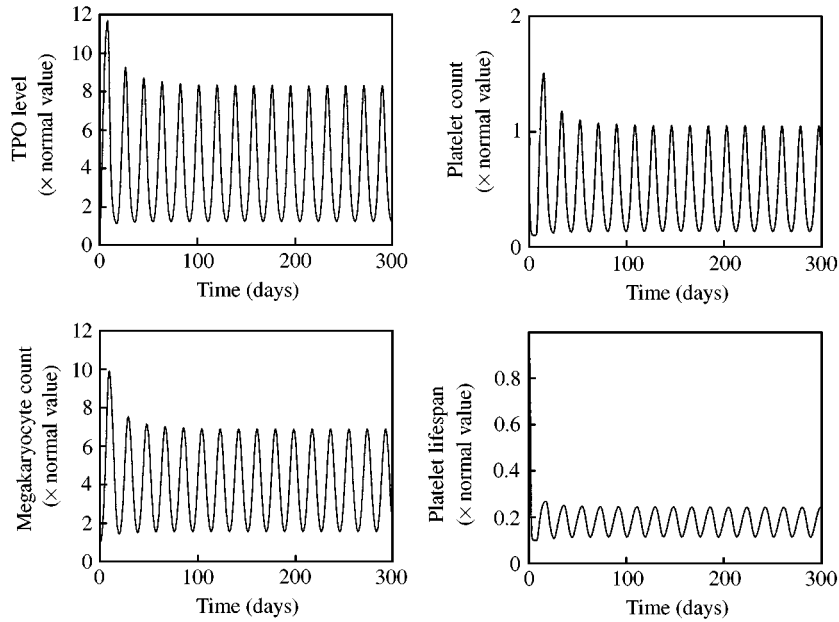
FIG. 11. As in Figs 9 and 10 except the platelet death rate is equal to 10.0 times the normal value ($\gamma \simeq 1.5$ day^{-1}). After a transient of about 100 days, the system reaches a state with sustained oscillations in all the variables. The TPO level and the megakaryocyte count oscillate from about normal to higher levels, the platelet count oscillates from low to slightly above normal values, and the platelet lifespan oscillates around a low value. The period of oscillation for all variables is about 18.8 days.
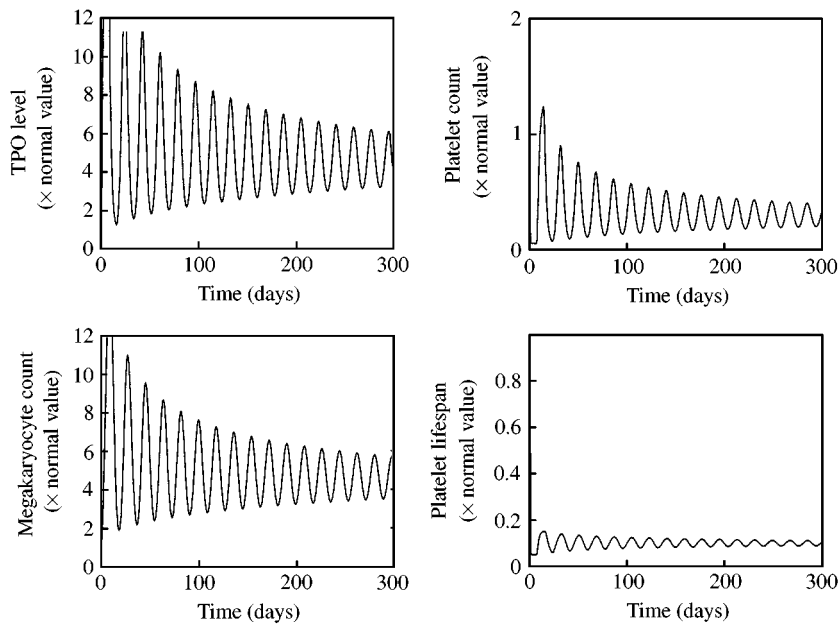
FIG. 12. Here the platelet death rate is equal to 20.0 times the normal value ($\gamma \simeq 3.0$ day^{-1}). No transient is discarded. In this case the system evolves towards a stable steady state where the platelet count and the platelet lifespan are decreased below their normal values, while the megakaryocyte count and the TPO level are increased above their normal values.

linear dependence of the megakaryocyte production rate on the TPO level, and ignores the stage of megakaryoblasts between the stem cells and the megakaryocytes. Although the desire to simplify the model equations motivates taking into account three lumped megakaryocyte classes, all other assumptions were made because of the lack of sufficient experimental data. For

instance, there is evidence that TPO affects the aging velocity of both platelets and megakaryocytes, but this has not been measured quantitatively. It is also known that stem cells pass through the stage of megakaryoblasts before becoming megakaryocytes, and that this stage lasts around 3 days. However, there is not enough experimental information about the dynamics of the megakaryoblast population to include their dynamics in a model such as ours at the present time. For these reasons we assumed constant aging velocities and that new megakaryocytes are produced with a velocity proportional to the TPO level, ignoring a possible delay due to the megakaryoblast compartment. It is our premise that despite these assumptions, the model takes into account the essentials of the system.

Special attention was given to the estimation of all the model parameters. Whenever possible, human data were employed. Unfortunately, that was not always possible, and in some cases we had to use data from sheep and mice, and even *in vitro* data in our determination of the rates of movement between megakaryocyte classes $[k_0(T)$ and $k_1(T)]$. For this reason we believe that the values estimated for these parameters are not as good as the others. This may explain why the experimental response of the platelet count after a injection of TPO is slightly different from that predicted by the model, in the interval from 5 to 10 days after the injection (see Fig. 8). While the experiment reveals that an increment of the platelet count can be noticed as soon as 5 days after the injection, it takes around 7 days for the model response to be noticed. Seven days is the megakaryocyte maturation time. Therefore, the model response is not noticed until the megakaryocytes produced immediately after the injection mature and release platelets. In other words, an increment in the platelet production rate due to the shift of megakaryocytes to higher ploidy classes, in response to the increased TPO level, is not observed. This may be due to the consideration of only three lumped megakaryocyte classes or to a underestimation of the megakaryocyte class shifting rates $[k_0(T)$ and $k_1(T)]$.

As seen in Fig. 8, numerical solutions of the model reproduce the normal response of the platelet count and the TPO level after a bolus injection of TPO, as measured by Harker *et al.*

(2000). The model also shows that an increase in the platelet death rate into the range from $\gamma \simeq 0.35$ to $1.65\ \mathrm{day}^{-1}$ causes a cyclic variation in platelet count, the megakaryocyte count, the TPO level, and the platelet lifespan. These resemble the symptoms of autoimmune cyclical thrombocytopenia, thought to be caused by a failure in the autoimmune system, which increases the platelet death rate.

The model presented here is capable of accounting for both the normal response to TPO injection and the consequences of elevated platelet destruction rates in producing the dynamic characteristics of autoimmune cyclical thrombocytopenia. We suspect that the amegakaryocytic version of cyclical thrombocytopenia, with its longer periods and different dynamic clinical presentation, will find an explanation in considerations of the dynamics of the hematopoietic stem cell. When possible destabilizing influences in the stem cell compartment are considered, the present model will play a valuable adjunct in studying the peripheral manifestation of these stem cell oscillations. Finally, we note that the present model will be of value in the study of dynamically timed TPO management of autoimmune-induced cyclical thrombocytopenia.

REFERENCES

ARANDA, E. & DORANTES, S. (1977). Garcia's disease: cyclic thrombocytopenic purpura in a child and abnormal platelet counts in his family. *Scand. J. Haematol.* **18,** 39–46.

BALDUINI, C., STELLA, C., ROSTI, V., BERTOLINO, G., NORIS, P. & ASCARI, E. (1993). Acquired cyclic thrombocytopenia thrombocytosis with periodic defect of platelet function. *Br. J. Haematol.* **85**, 718–722.

BÉLAIR, J. & MACKEY, M. (1987). A model for the regulation of mammalian platelet. *Ann. N. Y. Acad. Sci.* **504**, 280–282.

BÉLAIR, J., MACKEY, M. & MAHAFFY, J. M. (1995). Age-structured and two-delay models for erythropoiesis. *Math. Biosci.* **128**, 317–346.

BERNARD, J. & CAEN, J. (1962). Purpura thrombopenique et megacaryocytopenie cycliques mensuels. *Nouv. Rev. Franc. Hemat.* **2**, 378–386.

BEUTLER, E., LICHTMAN, M. A., COLLER, B. S. & KIPPS, T. J. (1995). *Williams Hematology*. New York: McGraw-Hill.

BORGE, O. J., RAMSFJELL, V., VEIBY, O. P., MURPHY, M. J., LOK, S. & JACOBSEN, S. E. (1996). Thrombopoietin, but not erythropoietin promotes viability and inhibits apoptosis of multipotent murine hematopoietic progenitor cells *in vitro. Blood* **88**, 2859–2870.

BORGE, O. J., RAMSFJELL, V., CUI, L. & JACOBSEN, S. E. (1997). Ability of early acting cytokines to directly promote survival and suppress apoptosis of human primitive CD34 + CD38- bone marrow cells with multilineage potential at the single cell level: key role of thrombopoietin. *Blood* **90**, 2282.

BRANEHOG, I., KUTTI, J., RIDELL, B., SWOLIN, B. & WEINFELD, A. (1975). The relation of thrombokinetics to bone marrow megakaryocytes in idiopathic thromobocytopenic purpura (ITP). *Blood* **45**, 552–562.

BREY, O., GARNER, E. P. R. & WELLS, D. (1969). Cyclic thrombocytopenia associated with multiple antibodies. *Br. Med. J.* **3**, 397–398.

BROUDY, V. C., LIN, N. L. & KAUSHANSKY, K. (1995). Thrombopoietin (*c*-mpl ligand) acts synergistically with erythropoietin, stem cell factor, and interleukin-11 to enhance murine megakaryocyte colony growth and increases megakaryocyte ploidy *in vitro. Blood* **85**, 1719–1726.

CAEN, J., MESHAKA, G., LARRIEU, M. J. & BERNARD, J. (1964). Les purpuras thrombopeniques intermittents idiopathiques. *Sem. Hop. Paris* **40**, 276–282.

CAMILLE, N. A. & MARSHALL, A. L. (1995). Structure of the marrow. In: *Williams Hematology* (Beutter, E., Marshall, A. L., Coller, B. S. & Kipps, T. J., eds), 5th Edn, pp. 25–37. New York: McGraw Hill.

CHINTAGUMPALA, M. M., HURTWITZ, R. L., MOAKE, J. L., MAHONEY, D. H. & STEUBER, C. P. (1992). Chronic relapsing thrombotic thrombocytopenic purpura in infants with large von Willebrand factor multimers during remission. *J. Pediatr.* **120**, 49–53.

COHEN, T. & COONEY, D. P. (1974). Cyclical thrombocytopenia: case report and review of literature. *Scand. J. Haematol.* **12**, 9–17.

DAN, K., INOKUCHI, K., AN, E. & NOMURA, T. (1991). Cell mediated cyclic thrombocytopenia treated with azathioprine. *Br. J. Haematol.* **77**, 365–379.

DEMMER, T. (1920). Morbus maculosus werlhofii in regelmassigen vierwochentlichen schuben bei einem 60 jahrigen mann, nebst untersuchungen uber die blutplattchen. *Folia Haematol.* **26**, 74–86.

EATON, D. L. & DE SAUVAGE, F. J. (1997). Thrombopoietin: the primary regulator of megakaryocytopoiesis and thrombopoiesis. *Exp. Hematol* **25**, 1–7.

ELLER, J., GYÖRI, I., ZOLLEI, J. & KRIZSA, F. (1987). Modelling thrombopoiesis regulation I: Model description and simulation results. *Comput. Math. Appl.* **14**, 841–848.

ELLIS, M. H., AVRAHAM, H. & GROOPMAN, J. E. (1995). The regulation of megakaryocytopoiesis. *Blood Rev.* **9**, 1–6.

ENGSTROM, K., LUNDQUIST, A. & SODERSTROM, N. (1966). Periodic thrombocytopenia or tidal platelet dysgenesis in a man. *Scand. J. Haematol.* **3**, 290–292.

FORTIN, P. & MACKEY, M. C. (1999). Periodic chronic myelogenous leukemia: spectral analysis of blood cell counts and etiological implications. *Br. J. Haematol.* **104**, 336–345.

GLASS, L. & MACKEY, M. C. (1988). *From Clocks to Chaos: The Rhythms of Life*. Princeton, NJ: Princeton University Press.

GOLDSCHMIDT, B. & FONO, R. (1972). Cyclic fluctuations in platelet count, megakaryocyte maturation and thrombopoietin activity in cyanotic congenital heart disease. *Acta Paediatr. Scand.* **61**, 310–314.

GRAY, W. M. & KIRK, J. (1971). Analysis by analogue and digital computers of the bone marrow stem cell and platelet control mechanisms. In: *Proc. Conf. Computers for Analysis and Control in Medical and Biological Research*, pp. 120–124. UK: IEE.

GYÖRI, I. & ELLER, J. (1987). Modelling thrombopoiesis regulation II: Mathematical investigation of the model. *Comput. Math. Appl.* **14**, 849–859.

HARKER, L. A., ROSKOS, L. K., MARZEC, U. M., CARTER, R. A., CHERRY, J. K., SUNDELL, B., CHEUNG, E. N., TERRY, D. & SHERIDAN, W. (2000). Effects of megakaryocyte growth and development factor on platelet production, platelet lifespan, and platelet function in normal human volunteers. *Blood* **95**, 2514–2529.

HAURIE, C., DALE, D. C. & MACKEY, M. C. (1998). Cyclical neutropenia and other periodic hematological diseases: a review of mechanisms and mathematical models. *Blood* **92**, 2629–2640.

HAURIE, C., DALE, D. C. & MACKEY, M. C. (1999a). Occurrence of periodic oscillations in the differential blood counts of congenital, idiopathic and cyclical neutropenic patients before and during treatment with G-CSF. *Exp. Hematol.* **27**, 401–409.

HAURIE, C., PERSON, R., DALE, D. C. & MACKEY, M. C. (1999b). Haematopoietic dynamics in grey collies. *Exp. Hematol.* **27**, 1139–1148.

HAURIE, C., DALE, D. C., RUDNICKI, R. & MACKEY, M. C. (2000). Modeling complex neutrophil dynamics in the grey collie. *J. theor. Biol.* **204**, 505–519.

HEARN, T., HAURIE, C. & MACKEY, M. C. (1998). Cyclical neutropenia and the peripheral control of white blood cell production. *J. theor. Biol.* **192**, 167–181.

HOFFBRAND, A. V. & PETIT, J. F. (1993). *Essential Haematology*, 3rd Edn. Oxford: Blackwell.

HOFFMAN, R., BRIDELL, R. A., VAN BESIEN, K., SROUR, E. F., GUSCAR, T., HUDSON, N. W. & GANSER, A. (1989). Acquired cyclic amegakaryocytic thrombocytopenia associated with an immunoglobulin blocking the action of granulocyte-macrophage colony-stimulating factor. *N. Engl. J. Med.* **321**, 97–102.

KAUSHANSKY, K. (1995). Thrombopoietin: the primary regulator of platelet production. *Blood* **86**, 419–431.

KAUSHANSKY, K., BROUDY, V. C., LIN, N., JORGENSEN, M. J., MCCARTY, J., FOX, N., ZUCKER-FRANKLIN, D. & LOFTON-DAY, C. (1995). Thrombopoietin, the Mpl ligand, is essential for full megakaryocyte development. *Proc. Natl. Acad. Sci. U.S.A.* **92,** 3234–3238.

KIMURA, F., NAKAMURA, Y., SATO, K., WAKIMOTO, N., KATO, T., TAHARA, T., YAMADA, M., NAGATA, N. & MOTOYOSHI, K. (1996). Cyclic change of cytokines in a patient with cyclic thrombocytopenia. *Br. J. Haematol.* **94,** 171–174.

KIRK, J., ORR, J. S. & HOPE, C. S. (1968). A mathematical analysis of red blood cell and bone marrow stem cell control mechanisms. *Br. J. Haematol.* **15,** 35–46.

KUTER, D. J. (1996). The physiology of platelet production. *Stem Cells* **14,** 88–101.

KUTER, D. J. & ROSENBERG, R. D. (1995). The reciprocal relationship of thrombopoietin (c-Mpl ligand) to changes in the platelet mass during busulfan induced thrombocytopenia in the rabbit. *Blood* **85,** 2720–2730.

KUTER, D. J., HUNT, S. & ZUCKER-FRANKLIN, D. (1997). *Thrombopoiesis and Thrombopoietins.* Totowa, New Jersey: Humana Press.

KUTER, D. J., MIYAZAKI, H. & KATO, T. (1997). The purification of thrombocytopenic plasma. In: *Thrombopoiesis and Thrombopoietins. Molecular, Cellular, Preclinical and Clinical Biology.* (Kuter, D. J., Hunt, P., Sheridan, W. & Zucker-Franklin, D., eds), pp. 143–164. Totowa, New Jersey: Humana Press.

LAYTON, J. E., HOCKMAN, H., SHERIDAN, W. P. & MORSTYN, G. (1989). Evidence for a novel *in vivo* control mechanism of granulopoiesis: mature cell-related control of a regulatory growth factor. *Blood* **74,** 1303–1307.

LEWIS, M. L. (1974). Cyclic thrombocytopenia: a thrombopoietin deficiency. *J. Clin. Pathol.* **27,** 242–246.

MACKEY, M. C. (1978). A unified hypothesis for the origin of aplastic anemia and periodic haematopoiesis. *Blood* **51,** 941–956.

MACKEY, M. C. (1979a). Dynamic haematological disorders of stem cell origin. In: *Biophysical and Biochemical Information Transfer in Recognition,* (Vassileva-Popova, J. G. & Jensen, E. V., eds), pp. 373–409. New York: Plenum Publishing Corp.

MACKEY, M. C. (1979b). Periodic auto-immune hemolytic anemia: an induced dynamical disease. *Bull. Math. Biol.* **41,** 829–834.

MACKEY, M. C. (1996). Mathematical models of hematopoietic cell replication and control. In: *The Art of Mathematical Modeling: Case Studies in Ecology, Physiology and Biofluids* (Othmer, H. G., Adler, F. R., Lewis, M. A. & Dallon, J. C., eds), pp. 149–178. New York: Prentice-Hall.

MACKEY, M. C. & GLASS, L. (1977). Oscillation and chaos in physiological control systems. *Science* **197,** 287–289.

MAHAFFY, J. M., BÉLAIR, J. & MACKEY, M. (1998). Hematopoietic model with moving boundary condition and state dependent delay: applications in erythropoiesis. *J. theor. Biol.* **190,** 135–146.

MORLEY, A. (1969). A platelet cycle in normal individuals. *Aust. Ann. Med.* **18,** 127–129.

ORR, J. S., KIRK, J., GRAY, K. G. & ANDERSON, J. R. (1968). A study of the interdependence of red cell and bone marrow stem cell populations. *Br. J. Haematol.* **15,** 23–24.

PAPAYANNOPOULOU, T. (1996). Biologic effects of thrombopoietin, the Mpl ligand, and its therapeutic potential. *Cancer Chemother. Pharmacol.* **38,** S69–S73.

PENNINGTON, D. G., STREATFIELD, K. & ROXBURY, A. E. (1979). Megakaryocytes and heterogeneity of circulating platelets. *Br. J. Haematol.* **34,** 639–653.

RATAJCZAK, M. Z., RATAJCZAK, J. MARLICZ, W., PLETCHER, C. H., MACHALINSKI, B., MOORE, J., HUNG, H. & GEWIRTZ, A. M. (1997). Recombinant human thrombopoietin (TPO) stimulates erythropoiesis by inhibiting erythroid progenitor cell apoptosis. *Br. J. Haematol.* **98,** 8–17.

RITCHIE, A., VADHAN-RAJ, S. & BROXMEYER, H. E. (1996). Thrombopoietin suppresses apoptosis and behaves as a survival factor for the human growth factor-dependent cell line, M07e. *Stem Cells.* **14,** 330–336.

RITCHIE, A., GOTOH, A., GADDY, J., BRAUN, S. E. & BROXMEYER, H. E. (1997). Thrombopoietin upregulates the promoter conformation of p53 in a proliferation-independent manner coincident with a decreased expression of bax: potential mechanisms for survival enhancing effects. *Blood* **90,** 4394–4402.

SITNICKA, E., LIN, N., PRIESTLEY, G. V., FOX, N., BROUDY, V. C., WOLF, N. S. & KAUSHANSKY, K. (1996). The effect of thrombopoietin on the proliferation and differentiation of murine hematopoietic stem cells. *Blood* **87,** 4998–5005.

SKOOG, W. A., LAWRENCE, J. S. & ADAMS, W. S. (1957). A metabolic study of a patient with idiopathic cyclical thrombocytopenic purpura. *Blood* **12,** 844–856.

SOLAR, G. P., KERR, W. G., ZEIGLER, F. C., HESS, D., DONAHUE, C., DE SAUVAGE, F. J. & EATON, D. L. (1998). Role of c-Mpl in early hematopoiesis. *Blood* **92,** 4–10.

SULSKY, D. (1994). Numerical solution of structured population models: Ii mas structure. *J. Math. Biol.* **32,** 491–514.

SWINBURNE, J. & MACKEY, M. C. (2000). Cyclical thrombocytopenia: characterization by spectral analysis and a review. *J. Theor. Med.* **2,** 81–91.

TANIMUKAI, S., KIMURA, T., SAKABE, H., OHMIZONO, Y., KATO, T., MIYAZAKI, H., YAMAGISHI, H. & SONODA, Y. (1997). Recombinant human c-Mpl ligand (thrombopoietin) not only acts on megakaryocyte progenitors, but also on erythroid and multipotential progenitors *in vitro. Exp. Hematol.* **25,** 1025–1033.

TEFFERI, A., SOLBERG, L. A., PETITT, R. M. & WILLIS, L. G. (1989). Adult onset cyclic bicytopenia: a case report and review of treatment of cyclic hematopoiesis. *Am. J. Hematol.* **30,** 181–185.

VADAN-RAJ, S., MURRAY, L. J., BUESO-RAMOS, C., PATEL, S., REDDY, S. P., HOOTS, W. K., JOHNSTON, T., PAPADOPOLOUS, N. E., HITTELMAN, W. N., JOHNSTON, D. A., YANG, T. A., PATON, V. E., COHEN, R. L., HELLMANN, S. D., BENJAMIN, R. S. & BROXMEYER, H. E. (1997). Simulation of megakaryocyte and platelet production by a single dose of human recombinant thrombopoietin in patients with cancer. *Ann. Intern. Med.* **126,** 673–681.

VON SCHULTHESS, G. K. & GESSNER, U. (1986). Oscillating platelet counts in healthy individuals: experimental investigation and quantitative evaluation of thrombocytopoietic feedbak control. *Scand. J. Haematol.* **36,** 473–479.

WASASTJERNA, C. (1967). Cyclic thrombocytopenia of acute type. *Scand. J. Haematol.* **4,** 380–384.

WICHMANN, H. E., GERHARDTS, M. D., SPECHTMEYER, H. & GROSS, R. (1979). A mathematical model of thrombopoiesis in the rat. *Cell Tissue Kinet.* **12**, 551–567.

WILKINSON, T. & FIRKIN, B. (1966). Idiopathic cyclical acute thrombocytopenic purpura. *Med. J. Aust.* **1**, 217–219.

YAGI, M., RITCHIE, K. A., SITNICKA, E., STOREY, C. & ROTH, G. J. (1999). Sustaines *ex vivo* expansion of hematopoietic stem cells mediated by thrombopoietin. *Proc. Natl. Acad. Sci. U.S.A.* **96**, 8126–8131.

YANABU, M., NOMURA, S., FUKUROI, T., KAWAKATSU, T., KIDO, H., YAMAGUCHI, K., SUZUKI, M., KOKAWA, T. & YASUNAGA, K. (1993). Periodic production of antiplatelet autoantibody directed against GP IIIa in cyclic thrombocytopenia. *Acta Haematol.* **89**, 155–159.

ZAULI, G., VITALE, M., FALCIERI, E., GIBELLINI, D., BASSINI, A., CELEGHINI, C., COLUMBARO, M. & CAPITANI, S. (1997). *In vitro* senescence and apoptotic cell death of human megakaryocytes. *Blood* **90**, 2234–2243.

ZEIGLER, F. C., DE SAUVAGE, F., WIDMER, H. R., KELLER, G. A., DONAHUE, C., SCHREIBER, R. D., MALLOY, B., HASS, P., EATON, D. & MATTHEWS, S. W. (1994). *In vitro* megakaryocytopoietic and thrombopoietic activity of c-Mpl ligand (TPO) on purified murine hematopoietic stem cells. *Blood* **84**, 4045–4052.

APPENDIX A

Numerical Methods

The platelet model described in Section 3 is a system of partial differential equations that is solved numerically following the techniques of Sulsky (1994) by integrating along the characteristics. Since the aging velocities $V(T)$ and W are both assumed to be constant and equal to unity, the age-structured populations move in constant steps with time, so the characteristic curves are straight lines with unitary slope. This permits the following discretization of the model's variables:

$$T_i = T(t_i), \quad m_{ij}^{(n)} = m_n(t_i, \mu_j), \quad n = 0, 1, 2,$$

$$\text{and} \quad p_{ik} = p(t_i v_k)$$

with $t = t_0 + ih$, h being a step size in time and, μ_j and v_k are appropriate age-structure grids. The index j in μ_j moves between 0 and $M_\mu = \mu_F/h$. The lower limit for the index k in v_k is also 0, but its upper limit is not fixed and is given by $M_v(i) = v_F(t_i)/h$. In general, $\mu_j = jh$ and $v_k = kh$, except for the last point in the second case, which depends on the boundary condition given by eqn (11).

In all the numerical experiments presented, the variables are initiated with their corresponding normal steady-state values. The numerical routine begins by integrating eqn (12) using the improved Euler's method to find the new TPO concentration T_i. The method of characteristics is used for subsequent calculations of the megakaryocyte and mature platelets calculations. The megakaryocyte populations are written as

$$m_{ij}^{(0)} = m_{i-1\,j-1}^{(0)} - hk_{01}(T_i)\, m_{i-1\,j-1}^{(0)},$$

$$m_{ij}^{(1)} = m_{i-1\,j-1}^{(1)} + hk_{01}(T_i)\, m_{i-1\,j-1}^{(0)}$$

$$- hk_{12}(T)m_{i-1\,j-1}^{(1_i)}$$

and

$$m_{ij}^{(2)} = m_{i-1\,j-1}^{(2)} + hk_{12}(T_i)m_{i-1\,j-1}^{(1)},$$

for all values of j except $j = 0$ where the boundary conditions given by eqns (2) and (3) are employed: $m_{i0}^{(0)} = S_0' T_i$, $m_{i0}^{(1)} = 0$, and $m_{i0}^{(2)} = 0$.

The platelet population obeys

$$p_{ij} = p_{i-1\,j-1}\, e^{\gamma h}$$

for all j's, except $j = 0$, where the boundary condition (3.9) is used. The age of the oldest platelets is determined by destroying a constant number Q of platelets, with the program finding how many mature classes remain, including any fractional remainder. Linear interpolation is used to find the new $v_F(t_i)$.

Finally, the total platelet count is calculated by integrating the platelet distribution population, using the trapezoid rule. With this new platelet count, a new TPO concentration can be calculated. This completes a time step in the simulation and allows the computation of all the variables by iterating the loop.

The convergence of the algorithm was tested empirically by varying the time step h. We found that $h = 0.01$ days represents a good compromise between speed and accuracy.